Catalytic cycles for isobutane isomerization over sulfated-zirconia catalysts

K.B. Fogash *, Z. Hong ** and J.A. Dumesic ***

Department of Chemical Engineering, University of Wisconsin, Madison, WI 53706, USA

Received 8 August 1998; accepted 12 October 1998

Reaction kinetic studies of isobutane isomerization over sulfated-zirconia catalysts were performed at 423 K. These catalysts show sustained rates of dihydrogen production that follow the same trend with time-on-stream as the rate of hydrocarbon production. Lower rates of dihydrogen production and correspondingly lower rates of hydrocarbon production are observed for catalysts dried at 773 K compared to samples dried at 588 K. It appears that sulfated-zirconia has the ability to generate olefins under reaction conditions, and this dehydrogenation reaction appears to be reversible, because increasing levels of dihydrogen in the feed suppress catalytic activity. These kinetic data can be described by a reaction scheme involving oligomerization/β-scission, isomerization and hydride transfer steps over acid sites, combined with dehydrogenation steps that generate olefins. The values of the rate constants for oligomerization steps over sulfated-zirconia are several orders of magnitude higher than for the corresponding steps over H-mordenite, whereas the rate constants for hydride transfer steps are similar for sulfated-zirconia and H-mordenite.

Keywords: butane, isomerization, sulfated-zirconia, acidity, dehydrogenation

1. Introduction

We have reported elsewhere that feed olefins initiate the isomerization of isobutane over H-mordenite samples which do not display dehydrogenation properties at 473 K, whereas isobutane isomerization over sulfated-zirconia at 423 K does not require the presence of feed olefins to achieve high catalytic activity [1,2]. In general, the isomerization of isobutane over H-mordenite can be viewed as being a surface chain reaction, in which the reaction is initiated by adsorption of olefins, although other initiation pathways are possible [3–5]. Propagation steps involve oligomerization, isomerization, β-scission, and hydride transfer reactions. The surface chain reaction is terminated, for example, by the formation of coke or by the production of higher molecular weight species (e.g., C_6-species). We will show in the present paper that the surface chain reaction scheme developed for isobutane isomerization over H-mordenite [1] can be extended to sulfated-zirconia by addition of initiation reactions that produce olefins. These initiation steps are treated as dehydrogenation processes [6–10], although the detailed nature of these steps is not a critical part of our analysis. In this manner, isobutane isomerization over sulfated-zirconia can be effectively described utilizing a bi-functional reaction scheme, consisting of a catalytic cycle for olefin generation and a series of acid-catalyzed reactions that form the surface chain reaction.

* Current address: Air Products and Chemicals, Inc., 7201 Hamilton Boulevard, Allentown, PA 18195-1501, USA.
** Current address: Exxon Chemical Company, 4500 Bayway Drive, Baytown, TX 77522, USA.
*** To whom correspondence should be addressed.

2. Experimental

The sulfated-zirconia catalyst utilized in this study was provided by MEI (Flemington, NJ) in the form of a sulfated $Zr(OH)_4$ precursor, which was heated to 848 K in 1.5 h and maintained at this temperature for 2 h in 100 cm^3 (NTP)/min of dry O_2 per gram of precursor. After activation, the catalyst was removed from the reactor and stored in a desiccator. This catalyst has a BET surface area of 98 m^2/g and a sulfur loading of 1.8% (w/w) (Galbraith Laboratories).

The details of the reaction kinetics measurements for isobutane isomerization are reported elsewhere [1,2]. Typically, 500 mg of catalyst and 250 mg of quartz particles were loaded in a quartz reactor and dried for 1 h at 588 K (SZ-588) or 773 K (SZ-773) in 65 cm^3 (NTP)/min of flowing, dry He (Liquid Carbonic). Reaction kinetics measurements for isobutane isomerization were conducted at 423 K for various values of weight-hourly space-velocities (WHSV) from 2.0 to 20.2 h^{-1} (10–100% isobutane, AGA 99.5% purity instrument grade), with the balance consisting of He and different amounts of H_2 at a total flow rate of 65 cm^3 (NTP)/min. The major impurities in the isobutane feed were n-butane, propane and isopentane, for which the kinetics data were corrected. The isobutane contained C_4-olefins at a level of approximately 40 ppm. These olefins were removed with a bed of calcined H-mordenite maintained at room temperature. The reaction products were analyzed with a Hewlett Packard 5890 gas chromatograph equipped with a flame ionization detector. Gas separation was achieved either by a 24 ft 5% DC-200 Chromosorb P-AW column (Alltech), held at 323 K; or by a 7 ft 0.19% picric acid on Graphpac-GC column (Alltech),

with temperature programming, i.e., column held at 323 K for 5 min, then ramped to 373 K at 10 K/min, and held at 373 K until the analysis was complete.

A thermal conductivity detector was used to detect dihydrogen produced by the catalyst. Argon was used as the carrier gas. Separation of permanent gases (e.g., He, H_2, N_2, O_2, and CO) was achieved by a Molecular Sieve 13X column (Alltech), held at 303 K. The column also separated the permanent gases from the hydrocarbons present in the gas sample.

3. Results

3.1. Kinetics of isobutane isomerization

Figure 1 shows the rates of hydrocarbon production versus time-on-stream for isobutane isomerization at 423 K in the absence of H_2 over SZ-588, for feeds consisting of 10 and 100% isobutane for which the feed olefins were either retained or removed. It can be seen that sulfated-zirconia is active for isobutane isomerization with and without olefins in the feed. In general, even without H_2 in the feed, isobutane isomerization over sulfated-zirconia at 423 K shows slow deactivation, and the rate of deactivation does not show a significant dependence on the isobutane concentration or on the presence of olefins in the feed. Furthermore, the olefinic impurities in the feed have little effect on the initial rate (at 3 min time-on-stream) of isobutane isomerization. However, the initial rate of isobutane isomerization increases as the concentration of isobutane increases. For example, for feeds containing 10% isobutane (with and without olefin impurities), the initial rate of hydrocarbon production is $\sim$0.5 μmol g^{-1} s^{-1}, and the initial rate increases to $\sim$1.4 μmol g^{-1} s^{-1} as the isobutane concentration increases to 100% (with and without olefin impurities). The slight decrease in catalytic activity observed in figure 1 may be related to coke formation and/or loss of sulfur. While we cannot definitively point to a particular mode of deactivation, it is important to note certain experimental observations. In one set of experiments, the reaction was allowed to proceed for 48 h; and subsequent analysis of the catalyst indicated a carbon content of 0.32 wt%, compared to 0.12 wt% for the fresh catalyst. In addition, no detectable amounts of H_2S ($\sim$1 ppm) were observed in the reactor effluent.

Figure 2 shows the rates of hydrocarbon production over SZ-588 at 423 K versus time-on-stream for various concentrations of H_2 in a 10% isobutane feed for which the olefinic impurities were removed. An increase in the concentration of feed H_2 suppresses the rate of hydrocarbon production. For example, while the initial rate of hydrocarbon production is 0.6 μmol g^{-1} s^{-1} in the absence of feed dihydrogen, the initial rate decreases from $\sim$0.2 to $\sim$0.01 μmol g^{-1} s^{-1} when the concentration of feed H_2 increases from 15 to 90%. It is important to note that H_2 affects the reaction kinetics differently on sulfated-zirconia than on H-mordenite. As shown elsewhere [1], the presence of H_2 in the feed has little effect on the catalytic activity for isobutane isomerization at 473 K over H-mordenite. At higher temperatures, however, hydrogen may affect catalytic activity over H-mordenite via hydrogenation reactions with butylene intermediates [4,11,12].

Figure 3 shows the rates of hydrocarbon production over SZ-588 at 423 K versus time-on-stream for 0 and 90% H_2 in a 10% isobutane feed for which the olefinic impurities were either retained or removed. The presence of 5 ppm olefins in the feed did not appreciably change the rates of hydrocarbon production when H_2 was absent from the feed stream, while there appears to be a small promotional effect of feed olefins when 90% of the feed stream is H_2. For example, the initial rates of hydrocarbon production are $\sim$0.5 μmol g^{-1} s^{-1} with and without olefins in the feed when H_2 is absent from the feed stream; however, when

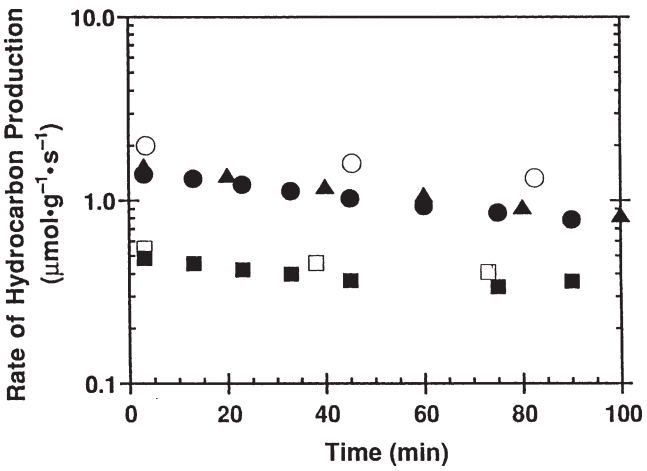

Figure 1. Rates of hydrocarbon production (μmol g^{-1} s^{-1}) versus time-on-stream for isomerization of isobutane over sulfated-zirconia (SZ-588) at 423 K for 10% isobutane in the feed with olefins present ((■) $\sim$5 ppm) and without olefins present (□), and for 100% isobutane in the feed with olefins present ((▲) $\sim$40 ppm, (●) $\sim$400 ppm) and without olefins present (○).

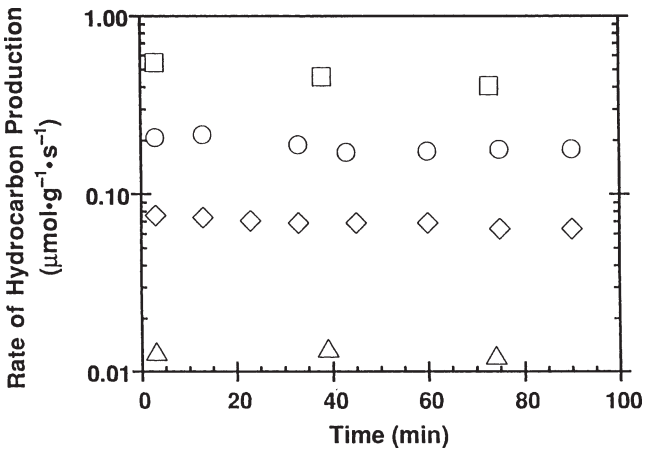

Figure 2. Effect of dihydrogen on the rates of hydrocarbon production versus time-on-stream for isobutane isomerization at 423 K over SZ-588 with 10% isobutane in the feed (without feed olefins) and H_2 concentrations of 0% (□), 15% (○), 50% (◇), and 90% (△), with the balance being helium.

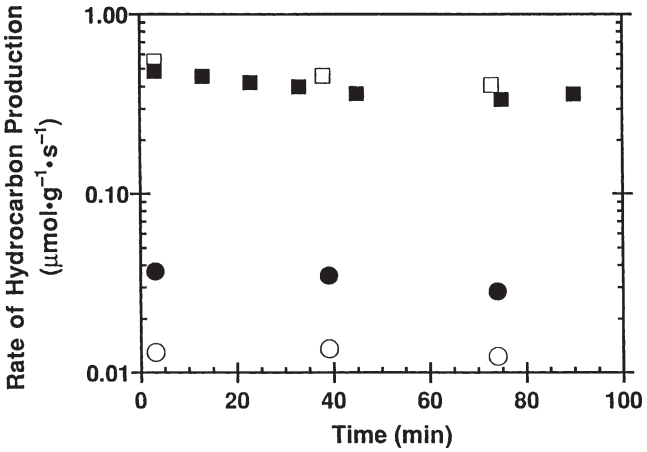

Figure 3. Effect of olefins on the rates of hydrocarbon production versus time-on-stream for isobutane isomerization over SZ-588 with 10% isobutane in the feed and no olefins present for 0% H_2 (□) and 90% H_2 (○); and for isobutane isomerization with 10% isobutane in the feed and ∼5 ppm of olefins present for 0% H_2 (■) and 90% H_2 (●).

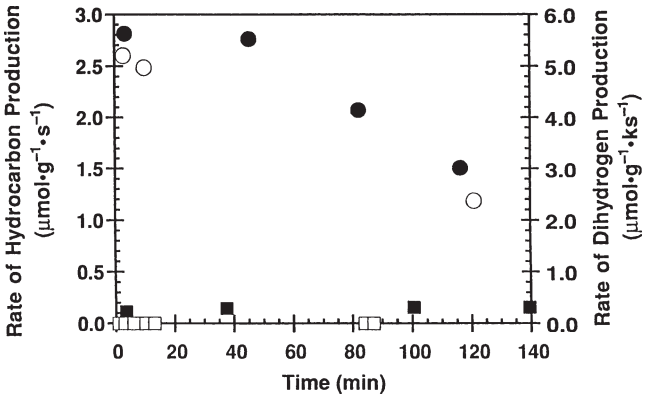

Figure 4. Rates of dihydrogen production (open symbols) and hydrocarbon production (filled symbols) versus time-on-stream for butane isomerization at 423 K with 100% butane in the feed over sulfated-zirconia dried at 588 and 773 K. Right axis: rates of dihydrogen production for SZ-588 (○) and SZ-773 (□). Left axis: rates of hydrocarbon production for SZ-588 (●) and SZ-773 (■).

the feed contains 90% H_2, the initial rate in the presence of feed olefins (∼0.04 μmol g^{-1} s^{-1}) is higher than the initial rate in the absence of feed olefins (∼0.02 μmol g^{-1} s^{-1}).

3.2. Evidence for in situ dehydrogenation processes

The fact that sulfated-zirconia is active for isobutane isomerization in the absence of feed olefins suggests that sulfated-zirconia may generate reactive intermediates *in situ* to initiate a surface chain reaction. One process to generate reactive intermediates may involve *in situ* dehydrogenation of isobutane to form dihydrogen and isobutylene, and the isobutylene can then adsorb onto acid sites to form reactive intermediates. Indeed, Sachtler and co-workers [6] have suggested that unpromoted sulfated-zirconia is able to produce butylene from butane. The details of the initiation processes of isobutane isomerization over sulfated-zirconia are discussed elsewhere [2]. Initiation may also occur via protolysis of isobutane [3,5,13] or by a redox process [9]. In short, we have observed that while isobutylene is consumed over sulfated-zirconia, dihydrogen (the other product of dehydrogenation of isobutane) is produced during isobutane isomerization at 423 K over SZ-588 and SZ-773. We have recently examined the initiation processes for butane isomerization using both experimental and DFT studies [2]. We should note that dihydrogen can also be produced by deposition of coke on the catalyst. However, we have observed that the rate of dihydrogen production during isomerization of n-butane is lower than during isomerization of isobutane, while the rate of catalyst deactivation caused by coke formation is faster during isomerization of n-butane. Therefore, we suggest that dihydrogen is produced primarily via the initiation step involving *in situ* dehydrogenation of isobutane.

Figure 4 shows the rates of hydrocarbon production as well as dihydrogen production versus time-on-stream for isobutane isomerization at 423 K over samples SZ-588 and SZ-773 for 100% isobutane feeds that do not contain olefinic impurities. As shown in figure 4, the rate of hydrocarbon production over the SZ-588 sample is ∼2.8 μmol g^{-1} s^{-1} at 3 min time-on-stream, and it gradually decreases to ∼1.6 μmol g^{-1} s^{-1} at 115 min time-on-stream. In parallel, the rate of H_2 production is ∼5.2 μmol g^{-1} ks^{-1} at 3 min time-on-stream, and it gradually decreases to ∼2.4 μmol g^{-1} ks^{-1} at 120 min time-on-stream. This result shows that the rates of hydrocarbon production and the rates of dihydrogen production follow the same trends with time for the SZ-588 sample. Moreover, for SZ-773 sample, lower dihydrogen production rates and correspondingly lower rates of hydrocarbon production are observed compared to those for SZ-588; therefore, the rates of dihydrogen production and isobutane isomerization appear to be linked. The primary difference between the two catalyst samples is that the sample dried at 588 K is more active for isobutane isomerization than the sample dried at 773 K. It should be noted that the rate of dihydrogen production is significantly lower than the rate of n-butane production, because dihydrogen is produced in an initiation step whereas n-butane is produced in the propagation steps of the surface chain reaction.

3.3. Reaction scheme for isobutane isomerization

The reaction scheme that we have used to describe isobutane isomerization over H-mordenite is based on acid-catalyzed reactions such as oligomerization, isomerization, β-scission, and hydride transfer. As noted earlier, the isomerization of isobutane over H-mordenite at 473 K is initiated for our reaction system by adsorption of feed olefins onto acid sites to form reactive intermediates [1]. This behavior of mordenite has, recently, been discussed by Engelhardt [3] and Guisnet and co-workers [11]. In view of the measurable catalytic activity for sulfated-zirconia in the absence of feed olefins and the observation of dihydrogen evolution by sulfated-zirconia under steady-state reaction

conditions, it appears that sulfated-zirconia has the ability to generate olefins and reactive intermediates under reaction conditions. Furthermore, this production of olefins and H_2 appears to be reversible, because increasing levels of H_2 in the feed suppress catalytic activity. Similar results were obtained at different reaction temperatures by Guisnet and co-workers [11] for n-butane isomerization. In general, the presence of H_2 has been shown to suppress catalytic activity for butane isomerization over sulfated-zirconia catalysts, e.g., [6,14]. Indeed, we have also observed isobutylene hydrogenation under reaction conditions. Furthermore, our microcalorimetric studies suggest that sulfated-zirconia does not strongly adsorb H_2 at 423 K. Thus, it appears that H_2 inhibits the isomerization reaction by converting the olefinic intermediates to alkanes, rather than by blocking acid sites involved in isomerization.

Figure 5 shows a simplified reaction scheme for isobutane isomerization over sulfated-zirconia at 423 K. The reaction is initiated by formation of isobutylene and H_2 through dehydrogenation of isobutane. The isobutylene formed in this manner adsorbs on an acid site (H–B) to form an isobutyl reactive intermediate. Reactive species are represented as protonated species associated with their conjugate bases on the surface. The extent of charge localization on the reactive intermediate is not specified here, e.g., whether the reactive intermediate is a carbenium ion (full charge transfer), a neutral surface alkoxy species, or a partially charged surface species. It should be noted, however, that recent quantum chemical studies, e.g., [15] suggest that the observable reaction intermediates on solid acid catalysts may resemble neutral alkoxy species, while the transition states for reactions of these intermediates may resemble positively charged carbenium ions.

The reactive intermediate can undergo various processes, including oligomerization, β-scission, and isomerization via a C_8 intermediate [11,14,16–23]. Eventually, an n-butyl reactive intermediate is formed on the surface, which can undergo hydride transfer with isobutane to form gaseous n-butane and an isobutyl reactive intermediate. The isobutyl reactive intermediate can then participate in further oligomerization, β-scission, and isomerization steps. Other reaction products can be produced via alternate oligomerization–cleavage pathways and hydride transfer steps.

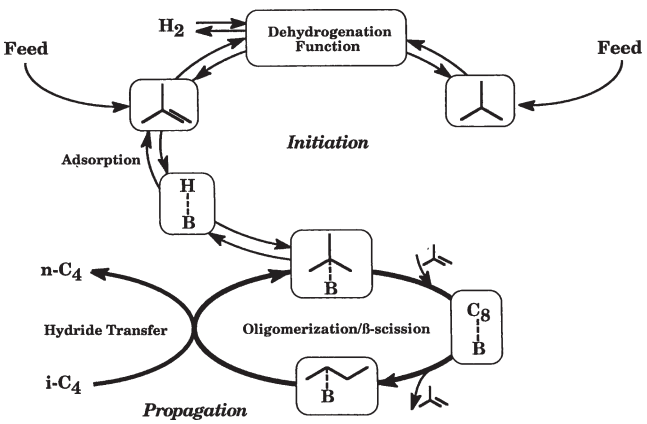

Figure 5. Simplified reaction scheme for isobutane isomerization over sulfated-zirconia at 423 K.

Figure 6 shows the 12-step model that was used to describe isobutane isomerization and disproportionation over sulfated-zirconia at 423 K. Importantly, steps 1–10 are the same steps that we have used to describe the conversion of isobutane over H-mordenite in the presence of feed olefins [1]. Adsorption/desorption of olefins on the acid sites is assumed to be quasi-equilibrated, and these steps are not shown explicitly. Steps 1–5 are oligomerization/β-scission steps, where the isomerization of C_8 and larger reactive intermediates is assumed to be rapid. Steps 1–3 are reversible, while steps 4–5 involving intermediates larger than C_8 are assumed to be irreversible. Hydride transfer steps are presented in steps 6–10, and these steps are considered to be irreversible, because isobutane is the only alkane present in high concentrations. Steps 11 and 12 represent the initiation steps in which isobutane undergoes dehydrogenation to form isobutylene and dihydrogen, and isobutylene subsequently adsorbs onto acid sites to form reactive intermediates. Our recent DFT studies [2] of the initiation processes for butane isomerization indicate the feasibility of step 11.

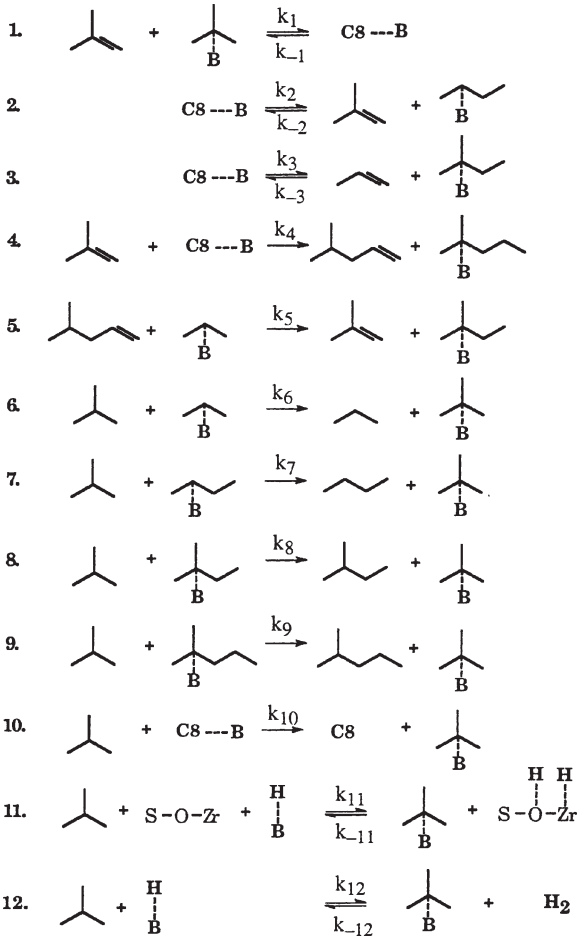

Figure 6. Representative reaction mechanism for isobutane isomerization and disproportionation over sulfated-zirconia at 423 K.

The oligomerization/β-scission steps are written as reactions of surface reactive intermediates with a gaseous olefin. Hydride transfer steps are also written as reactions of surface species with gaseous isobutane. However, the gaseous species in these steps are probably weakly adsorbed in precursor states prior to reaction with the surface species. It should be noted that only representative isomers are shown for the larger ($\geqslant C_5$) species, and the participation of other isomers is not precluded. Furthermore, the oligomerization/β-scission steps represent a series of steps involving oligomerization, hydride shifts, alkyl shifts, branching rearrangements, β-scission, and adsorption/desorption of the reactive intermediates. A more detailed description of these steps is presented elsewhere [1]. Because olefin adsorption/desorption is quasi-equilibrated, the formation of n-butylene and subsequent adsorption on an acid site is equivalent to formation of a n-butyl reactive intermediate. In either case, β-scission of the C_8 reactive intermediate forms isobutyl and n-butyl species, in agreement with mechanisms proposed over sulfated-zirconia [21,23].

3.4. Kinetic model for isobutane isomerization

A kinetic model was constructed based on the reaction steps of figure 6 to ascertain whether the surface chemistry represented in these steps can describe the quantitative trends exhibited by the reaction kinetics data. A more detailed discussion of the development of this type of kinetic model is presented elsewhere [1,24]. Briefly, the kinetic model involves estimation of rate or equilibrium constants for each step, which combined with steady-state relations for the reactive intermediates, are used to calculate surface coverages and rates of consumption and formation for the reactants and products of the reaction.

We start the analysis by determining reasonable values of the kinetic parameters. We do not require a unique set of parameters, since these values will be adjusted later in the analysis. Instead, we generate a feasible set of parameters that is consistent with the surface chemistry described in figure 6. This set of initial guesses for the kinetic parameters was reported elsewhere for isobutane conversion over H-mordenite [1], and we utilized this same set of initial guesses in the present study. These values were then used as initial guesses to fit the reaction kinetics data collected for sulfated-zirconia at 40 min time-on-stream. The reactor was assumed to be a plug-flow reactor. Table 1 shows the fitted rate constants for isobutane isomerization at 423 K over SZ-588. We estimated 95% confidence interval for each parameter assuming that the other parameters were constrained at the fitted values (i.e., we assumed a single-parameter, multi-response model), and the results of these calculations are also listed in table 1. The total fractional surface coverage ranged from 0.5 to 0.9 for the final rate constants. A comparison of the experimentally measured turnover frequencies (TOF) for production of butane, propane and pentane with the values predicted from the kinetic model is presented in table 2. The values of TOF were calculated assuming 75 μmol/g of active acid sites, as determined previously via selective poisoning studies [25]. Figures 7–9 illustrate that the trends displayed by the experimental data are properly described by the kinetic model, as outlined below.

Table 1
Rate constants with 95% confidence limits for isobutane isomerization at 423 K over sulfated-zirconia.

	k[a]
Step 1 (forward)	$(2.2 \pm 0.3) \times 10^5$
Step 1 (reverse)	0.12 ± 0.1
Step 2 (forward)	2.2 ± 0.5
Step 2 (reverse)	$(4.6 \pm 1.4) \times 10^6$
Step 3 (forward)	0.32 ± 0.1
Step 3 (reverse)	$(4.4 \pm 2) \times 10^5$
Step 4 (forward)	$(8.1 \pm 8) \times 10^3$
Step 5 (forward)	10^6 (insensitive)
Step 6 (forward)	0.67 ± 0.3
Step 7 (forward)	0.81 ± 0.3
Step 8 (forward)	$(4.4 \pm 2) \times 10^{-2}$
Step 9 (forward)	10^{-2} (insensitive)
Step 10 (forward)	10^{-4} (insensitive)
Step 11 (forward)	2×10^2 (insensitive)
Step 11 (reverse)	1 (insensitive)
Step 12 (forward)	$(2.8 \pm 0.4) \times 10^{-3}$
Step 12 (reverse)	4.2×10^{-4} [b]
K_{C_3}[c]	10^4
K_{C_4}[c]	10^5
K_{C_6}[c]	10^{10}

[a] Units of s^{-1} or $s^{-1}\,atm^{-1}$.
[b] Constrained by thermodynamics for isobutylene/isobutane equilibrium.
[c] Equilibrium constants (atm^{-1}) for adsorption of propylene, isobutylene, and C_6 olefins.

Table 2
Comparison of turnover frequencies, TOF (ks^{-1}), for production of butane, propane and pentane measured experimentally over sulfated-zirconia at 423 K and predicted from kinetic model.

Isobutane (atm)	Isobutylene (ppm)	Dihydrogen (atm)	TOF n-C_4 (ks^{-1})	TOF C_3 (ks^{-1})	TOF C_5 (ks^{-1})
Experimental values of TOF					
0.1	0	0	5.5	1.0	0.95
1.0	0	0	28.7	4.4	5.0
0.1	0	0.16	1.7	0.32	0.29
0.1	0	0.5	0.65	0.12	0.09
0.1	0	0.9	0.30	0.07	0.03
0.1	0	0.9	0.15	0.01	0.01
0.1	5	0	5.5	1.1	1.0
0.1	5	0.9	0.38	0.06	0.05
Predicted values of TOF					
0.1	0	0	5.9	1.1	1.1
1.0	0	0	23.8	5.4	5.4
0.1	0	0.16	1.5	0.33	0.33
0.1	0	0.5	0.40	0.07	0.07
0.1	0	0.9	0.18	0.03	0.03
0.1	0	0.9	0.17	0.03	0.03
0.1	5	0	5.9	1.1	1.1
0.1	5	0.9	0.21	0.03	0.03

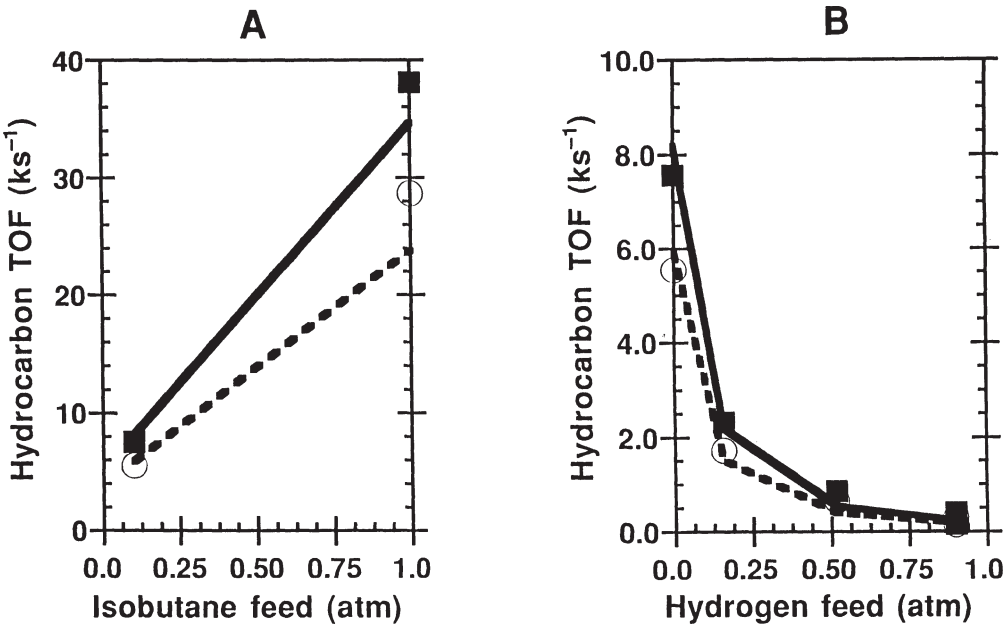

Figure 7. (A) Rates of total hydrocarbon production (■) and n-butane production (○) over SZ-588 at 423 K versus isobutane feed concentration. Results calculated from kinetic model are represented as solid (for total hydrocarbon) and dashed (for n-butane) lines. The remainder of the feed stream is helium. (B) Rates of total hydrocarbon production (■) and n-butane production (○) over SZ-588 at 423 K versus dihydrogen feed concentration. Results calculated from kinetic model are represented as solid (for total hydrocarbon) and dashed (for n-butane) lines. Isobutane pressure = 0.10 atm with the balance helium.

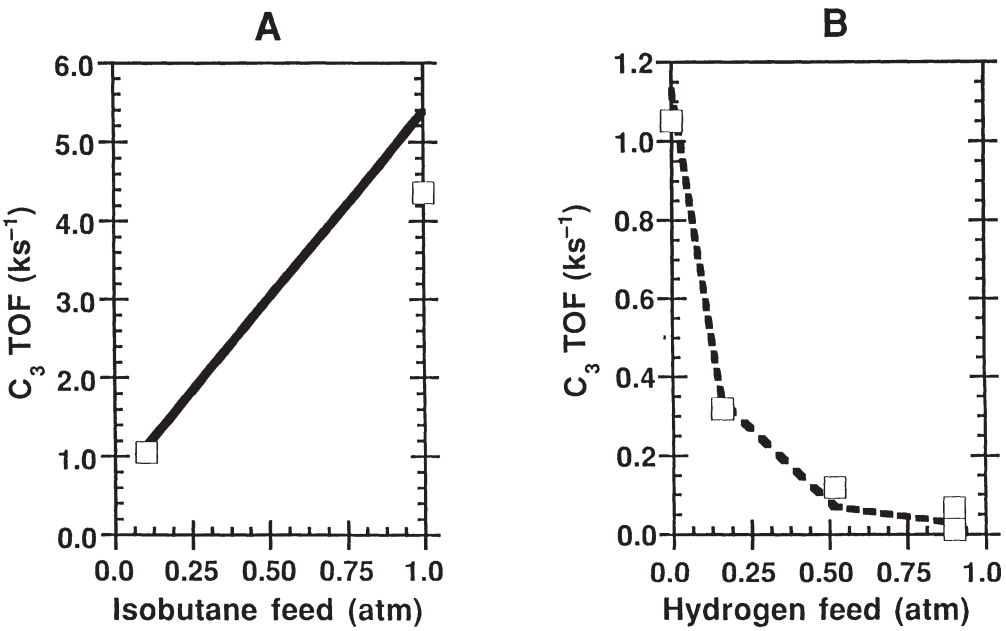

Figure 8. (A) Rates of C_3 production (□) over SZ-588 at 423 K versus isobutane feed concentration. Results calculated from kinetic model are represented as solid line. The remainder of the feed stream is helium. (B) Rates of C_3 production (□) over SZ-588 at 423 K versus dihydrogen feed concentration. Results calculated from kinetic model are represented as dashed line. Isobutane pressure = 0.10 atm with the balance helium.

Figure 7(A) shows the experimental and calculated turnover frequencies for productions of total hydrocarbons and n-butane versus the pressure of isobutane fed to the sulfated-zirconia catalyst at 423 K, with no H_2 in the feed. The fit obtained from the model appears to represent the production rates of total hydrocarbons and n-butane. Figure 7(B) shows the experimental and calculated turnover frequencies for productions of total hydrocarbons and n-butane versus the concentration of H_2 fed to the sulfated-zirconia catalyst at 423 K, with an isobutane pressure of ca. 0.10 atm. As the concentration of H_2 fed to the reactor is increased, the rates of production of total hydrocarbons and n-butane decrease over the sulfated-zirconia catalyst. The model appears to reproduce the experimental trend.

Figure 8(A) shows the experimental and calculated turnover frequencies for production of C_3-species versus

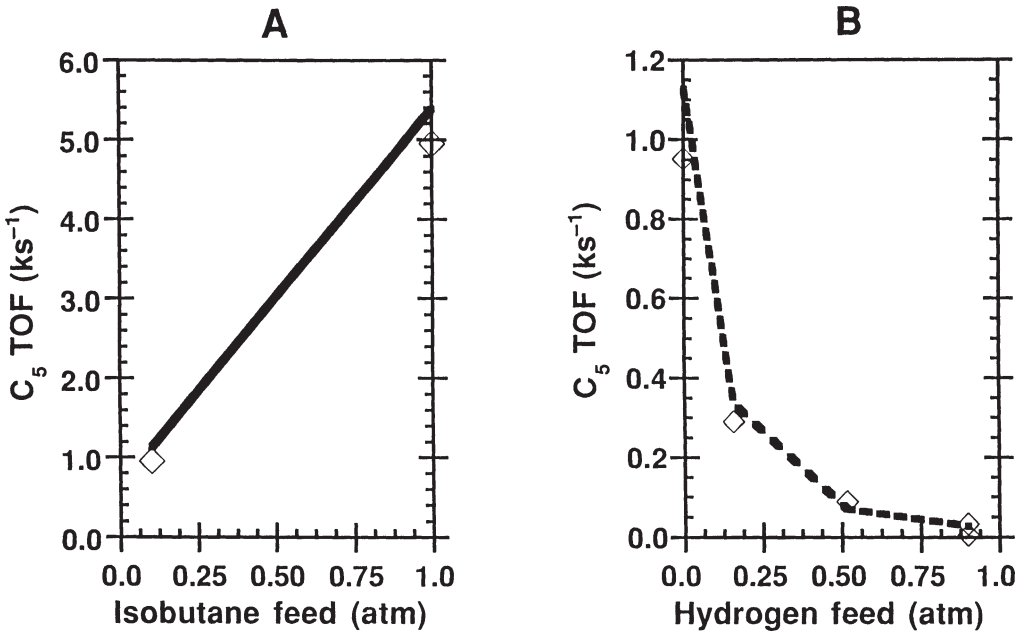

Figure 9. (A) Rates of C_5 production (◊) over SZ-588 at 423 K versus isobutane feed concentration. Results calculated from kinetic model are represented as solid line. The remainder of the feed stream is helium. (B) Rates of C_5 production (◊) over SZ-588 at 423 K versus dihydrogen feed concentration. Results calculated from kinetic model are represented as dashed line. Isobutane pressure = 0.10 atm with the balance helium.

the level of isobutane fed to the sulfated-zirconia catalyst at 423 K, with no H_2 in feed. The fit obtained from the model appears to describe the observed production rates of C_3-species. Figure 8(B) shows the experimental and calculated turnover frequencies of C_3 production versus the concentration of H_2 fed to the sulfated-zirconia catalyst at 423 K, with an isobutane pressure of ca. 0.10 atm. The rate of C_3 production decreases over the sulfated-zirconia catalyst as the concentration of H_2 fed to the reactor is increased. The model appears to reproduce the experimental trend.

Figure 9(A) shows the experimental and calculated turnover frequencies for production of C_5-species versus the level of isobutane fed to the sulfated-zirconia catalyst at 423 K, with no H_2 in feed. Figure 9(B) shows the experimental and calculated turnover frequencies for production of C_5-species versus the concentration of H_2 fed to the sulfated-zirconia catalyst at 423 K, with an isobutane pressure of 0.10 atm. The model captures the trends shown in these experimental data.

It can be seen in table 2 that the presence of 5 ppm of olefins in the feed increases slightly the rates of hydrocarbon production in the presence of H_2, while no measurable effect of feed olefins is detected in the absence of H_2. The model predicts a similar effect.

In the absence of feed olefins, rates of dihydrogen evolution of 5×10^{-5} and 5×10^{-3} μmol g^{-1} s^{-1} are detected in the reactor effluent for 10 and 100% isobutane in the feed, respectively. The model appears to reproduce the experimental trend of increasing dihydrogen evolution in the absence of feed olefins. For example, the model predicts that 6 and 30 ppm of H_2 would be present in the reactor effluent for 10 and 100% isobutane feeds, and the experimental values are ∼5 and ∼40 ppm, respectively.

4. Discussion

The major reaction pathways during isobutane conversion over sulfated-zirconia at our reaction conditions are isomerization to *n*-butane and disproportionation to propane and pentane. The observed distribution of the major products (C_3, n-C_4, and C_5) is consistent with that reported by others for isobutane isomerization over sulfated-zirconia [22,26].

Figures 7(A)–9(A) show that an increase in the isobutane feed concentration causes a higher level of hydrocarbon production. In addition, no significant change in the selectivity for n-butane is detected for different levels of isobutane. The presence of dihydrogen in the feed suppresses the rates of hydrocarbon production, as seen in figures 7(B)–9(B). However, there does not appear to be any significant change in the selectivity for n-butane production associated with an increase in the amount of dihydrogen in the feed. While addition of olefins increases slightly the rates of hydrocarbon production in the presence of dihydrogen, addition of olefins in the absence of dihydrogen does not affect the rates of hydrocarbon production. The primary effect of feed dihydrogen on the reaction scheme of figure 6 is on step 12. The remaining steps are altered indirectly by changes in the surface coverages caused by changes in the olefin production levels.

Dihydrogen and isobutylene are predicted, according to our kinetic model, to be in equilibrium with isobutane at the exit of the reactor when significant amounts of dihydrogen are in the feed; therefore, olefins present in the feed above

the equilibrium level would be hydrogenated, thereby eliminating any promotional effect of olefins in the feed. The small promotional effect that we observe associated with 5 ppm olefins in the presence of dihydrogen may result from reactions within the first ∼10% of the reactor bed, since dihydrogen and isobutylene are not in equilibrium with isobutane near the entrance to the reactor.

The rate of dihydrogen evolution and the rate of isobutane isomerization are both lower for the sulfated-zirconia catalyst dried at 773 K compared to the sample dried at 588 K. It has been reported by González et al. [27,28] that the primary difference between sulfated-zirconia catalysts dried at these two temperatures is that the sample dried at the lower temperature possessed more non-acidic hydroxyl groups that participate in hydrogen-bond interactions. Furthermore, the catalytic activity of the sample dried at 773 K can be promoted by dosing approximately 75 μmol/g of water onto the surface at 423 K. Accordingly, a moderate degree of catalyst hydration promotes butane isomerization over sulfated-zirconia. This promotional effect may be related to stabilization of the reactive intermediates by hydrogen bonding with the hydroxyl groups, thereby increasing the rate of isobutane dissociation and dehydrogenation [2].

Comparison of the rate constants obtained in the present study for isobutane isomerization over sulfated-zirconia at 423 K with the values determined elsewhere for H-mordenite at 473 K provides insight into the reaction pathways over these catalysts. While these rate constants were determined at different temperatures for these catalysts (i.e., at 423 K for sulfated-zirconia versus 473 K for H-mordenite), it is still possible to discern general trends regarding the relative rate constants for oligomerization, β-scission, and hydride transfer steps on the different catalysts.

The rate constants for the 10-step mechanism (steps 1–10 in figure 6) for isobutane isomerization over H-mordenite at 473 K are listed in table 3. These values for H-mordenite are slightly different from the values that we reported elsewhere [1], since we have re-analyzed our kinetic data for H-mordenite using a PFR model, to be consistent with our current analysis of sulfated-zirconia. In addition, we have modified the values of the parameters for the kinetically insensitive hydride transfer steps over H-mordenite such that these values show a monotonic trend with increasing hydrocarbon size.

Table 3
Ratio (τ) of sulfated-zirconia to H-mordenite fitted rate constants for isobutane isomerization.

	Rate constant[a] (H-mordenite)	Reaction type	Ratio
Step 1 (forward)	1.5×10^{3}	oligomerization	140
Step 1 (reverse)	1.3×10^{-1}	β-scission	0.94
Step 2 (forward)	1.3×10^{-1}	β-scission	17
Step 2 (reverse)	1.6×10^{4}	oligomerization	290
Step 3 (forward)	1.2×10^{-2}	β-scission	26
Step 3 (reverse)	1.1×10^{3}	oligomerization	400
Step 6 (forward)	1.3×10^{-1}	hydride transfer	5.1
Step 7 (forward)	1.3×10^{-1}	hydride transfer	6.2
Step 8 (forward)	4.3×10^{-2}	hydride transfer	1.0

[a] Units of s^{-1} or $s^{-1}\,atm^{-1}$.

We report in table 3 the ratio (τ) of kinetically significant rate constants for sulfated-zirconia to the corresponding rate constants for H-mordenite. It can be seen that the rate constants for oligomerization reactions over sulfated-zirconia are two orders of magnitude higher than the corresponding steps over H-mordenite, while the rate constants for β-scission reactions of those steps are similar for both catalysts. Accordingly, it appears that the equilibrium constants for surface oligomerization processes are shifted to favor higher molecular weight species on sulfated-zirconia compared to H-mordenite. The rate constants for the hydride transfer reactions over sulfated-zirconia are predicted to be essentially the same as the rate constants over H-mordenite. Steps 11 and 12 were not used in the H-mordenite reaction scheme because olefins were present in the feed stream and H-mordenite did not display dehydrogenation properties at 473 K for our reaction conditions.

The higher rate constants for oligomerization steps observed for sulfated-zirconia than for H-mordenite may reflect the closer proximity of active sites on sulfated-zirconia than on H-mordenite. These higher rate constants for sulfated-zirconia may also be caused by increased mobility of the reactive intermediates that participate in hydrogen bonding interactions with non-acidic hydroxyl groups. Importantly, the rate constants for hydride transfer reactions are approximately equivalent over both sulfated-zirconia and H-mordenite. This result is noteworthy, because sulfated-zirconia is an amorphous catalyst and H-mordenite is zeolitic in nature. While zeolites are known to exhibit high rates of hydride transfer [29,30], similar observations on amorphous materials have not been generally reported.

In general, it appears that the higher rate of isobutane isomerization over sulfated-zirconia at 423 K compared to H-mordenite at 473 K in the presence of feed olefins may be related to higher rate constants for oligomerization steps and comparable rate constants for β-scission and hydride transfer steps between the catalysts. Moreover, sulfated-zirconia is active in the absence of feed olefins because olefins are generated *in situ* via dehydrogenation processes.

5. Conclusions

The rates of hydrocarbon production and the rates of dihydrogen production follow the same trends with time-on-stream for sulfated-zirconia catalysts dried at 588 K. Furthermore, lower rates of hydrocarbon production and correspondingly lower rates of dihydrogen production are observed for the catalyst dried at 773 K compared to the sample dried at 588 K. This production of dihydrogen and the observation that sulfated-zirconia is active for isobutane isomerization in the absence of feed olefins suggest that sulfated-zirconia has the ability to generate olefins under

reaction conditions. This dehydrogenation reaction appears to be reversible, because increasing levels of dihydrogen in the feed stream suppress catalytic activity.

A reaction scheme that was developed elsewhere for isobutane isomerization over H-mordenite can be extended, with minor modifications, to describe isobutane isomerization over sulfated-zirconia. This 12-step model involves oligomerization/β-scission, hydride transfer, and dehydrogenation steps. Comparison of the rate constants for isobutane isomerization over sulfated-zirconia to values of the rate constants over H-mordenite shows that the rate constants for oligomerization reactions over sulfated-zirconia are two orders of magnitude higher than those values for the corresponding steps over H-mordenite. The rate constants for β-scission and hydride transfer reactions over sulfated-zirconia are similar to those values over H-mordenite.

Acknowledgement

We wish to acknowledge funding for this work from the Office of Basic Energy Sciences of the US Department of Energy. We also wish to thank Dr. R.D. Cortright for valuable discussions regarding analysis of our reaction kinetics data.

References

[1] K.B. Fogash, Z. Hong and J.A. Dumesic, J. Catal. 173 (1998) 519.
[2] Z. Hong, K.B. Fogash, R.M. Watwe, B. Kim, B.I. Mosqueda-Jimenez, M.A. Natal-Santiago, J.M. Hill and J.A. Dumesic, J. Catal. (1998), accepted.
[3] J. Engelhardt, J. Catal. 164 (1996) 449.
[4] M. Guisnet and N.S. Gnep, Appl. Catal. A 146 (1996) 33.
[5] J. Engelhardt and W.K. Hall, J. Catal. 125 (1990) 472.
[6] H. Liu, V. Adeeva, G.D. Lei and W.M.H. Sachtler, J. Mol. Catal. A 100 (1995) 35.
[7] D. Farcasiu, 214th National Meeting, Am. Chem. Soc., Las Vegas, NV, September (1997) 745.
[8] D. Farcasiu, A. Ghenciu and G. Miller, J. Catal. 134 (1992) 118.
[9] D. Farcasiu, A. Ghenciu and J.Q. Li, J. Catal. 158 (1996) 116.
[10] D. Farcasiu and A. Ghenciu, Progr. NMR Spectroscopy 29 (1996) 129.
[11] M. Trung Tran, N.S. Gnep, M. Guisnet and P. Nascimento, Catal. Lett. 47 (1997) 57.
[12] C. Bearez, F. Chevalier and M. Guisnet, React. Kinet. Catal. Lett. 22 (1983) 405.
[13] T. Cheung, F.C. Lange and B.C. Gates, Catal. Lett. 34 (1995) 351.
[14] V. Adeeva, G.D. Lei and W.M.H. Sachtler, Catal. Lett. 33 (1995) 135.
[15] A.M. Rigby, G.J. Kramer and R.A. van Santen, J. Catal. 170 (1997) 1.
[16] V. Adeeva, H.Y. Liu, B.Q. Xu and W.M.H. Sachtler, Topics Catal. 6 (1998) 61.
[17] V. Adeeva, G.D. Lei and W.M.H. Sachtler, Appl. Catal. A 118 (1994) L11.
[18] C. Bearez, F. Avendano, F. Chevalier and M. Guisnet, Bull. Soc. Chim. Fr. 3 (1985) 346.
[19] M.R. Guisnet, Acc. Chem. Res. 23 (1990) 392.
[20] T.K. Cheung, J.L. d'Itri and B.C. Gates, J. Catal. 151 (1995) 464.
[21] K.B. Fogash, R.B. Larson, M.R. Gonzalez, J.M. Kobe and J.A. Dumesic, J. Catal. 163 (1996) 138.
[22] A.S. Zarkalis, C.Y. Hsu and B.C. Gates, Catal. Lett. 37 (1996) 1.
[23] J.E. Tábora and R.J. Davis, J. Catal. 162 (1996) 125.
[24] G. Yaluris, J.E. Reskoske, L.M. Aparicio, R.J. Madon and J.A. Dumesic, J. Catal. 153 (1995) 54.
[25] G. Yaluris, R.B. Larson, J.M. Kobe, M.R. González, K.B. Fogash and J.A. Dumesic, J. Catal. 158 (1996) 336.
[26] A.S. Zarkalis, C.Y. Hsu and B.C. Gates, Catal. Lett. 29 (1994) 235.
[27] M.R. González, K.B. Fogash, J.M. Kobe and J.A. Dumesic, Catal. Today 33 (1997) 303.
[28] M.R. González, J.M. Kobe, K.B. Fogash and J.A. Dumesic, J. Catal. 160 (1996) 290.
[29] B.C. Gates, *Catalytic Chemistry* (Wiley, New York, 1992).
[30] P.B. Venuto, Micropor. Mater. 2 (1994) 297.